

MULTI-OBJECTIVE OPTIMIZATION OF A LOW-TEMPERATURE TRANSCRITICAL ORGANIC RANKINE CYCLE FOR WASTE HEAT RECOVERY

Lecompte S.^{1,2*}, Lazova, M.¹, van den Broek M.^{1,2}, De Paepe M.¹

*Author for correspondence

¹Department of Flow Heat and Combustion Mechanics, ² Department of Industrial System and Product Design,
 Ghent University, Ghent University,
 Gent, 9000, Kortrijk, 8500,
 Belgium, Belgium,

E-mail: steven.lecompte@ugent.be

ABSTRACT

The subcritical Organic Rankine Cycle (SCORC) is widely recognized as a viable technology for converting waste heat to electricity. However, a relative large exergy share is destroyed in the evaporator because of the subcritical heat exchange process. A transcritical cycle has the potential to reduce these irreversibilities in detriment of a financial cost. Therefore the inclusion of financial parameters is crucial for a sound comparison. First, a thermo-hydraulic sizing model for the supercritical ORC is developed. Second, from this model a thermo-economic analysis is provided based on a multi-objective optimization. The Pareto front of net power output versus investment costs are compared for the subcritical and transcritical ORC. Also a single objective criterion, the minimum specific investment cost, is calculated. The results can be used as a guideline to the design of new ORCs.

INTRODUCTION

The subcritical Organic Rankine Cycle (SCORC) is known as a viable technology for converting waste heat into electricity. The benefits of using an ORC are: low maintenance, autonomous operation, favourable operating pressures and the opportunity to recuperate low temperature waste heat. Still, there is potential for increased performance by considering advanced cycle designs like the transcritical ORC (TCORC).

In a TCORC, heat absorption occurs in a supercritical state, while condensation occurs in the usual two-phase region. The major difference with a subcritical ORC is the heating process of the working fluid. The working fluid is compressed directly to supercritical pressure and heated to a supercritical state, effectively bypassing the isothermal two-phase region. The transcritical cycle therefore has the potential to reduce exergy destruction in the evaporator.

The thermodynamic performance benefits of a transcritical cycle were early on investigated by among others Angelino and Colonna [1], Saleh et al. [2] and Schuster et al. [3].

NOMENCLATURE

C_p	[J/(kgK)]	Specific heat at constant pressure
\bar{C}_p	[J/(kgK)]	Averaged specific heat $(h_w - h_b)/(T_w - T_b)$
D_h	[m]	Hydraulic diameter
f	[-]	Friction factor
G	[kg/(m ² s)]	Mass flux
h	[J/kg]	Enthalpy
K	[-]	Number of paths
k	[W/(mK)]	Thermal conductivity
\dot{m}	[kg/s]	Mass flow rate
N		Number of passes
Nu	[-]	Nusselt number
p	[Pa]	Pressure
p_{co}		Corrugation pitch
PP	[°C]	Pinch point temperature difference
$SCORC$		Subcritical Organic Rankine Cycle
SIC	[€/kW]	Specific investment cost
T	[°C]	Temperature
t	[m]	Plate thickness
$TCORC$		Transcritical Organic Rankine Cycle
U	[W/(m ² K)]	Overall heat transfer coefficient
\dot{W}	[W]	Power
\dot{Q}	[W]	Heat transfer rate
Re	[-]	Reynolds number
Special characters		
α	[W/(m ² K)]	Convective heat transfer coefficient
β	[°]	Chevron angle
μ	[Pa.s]	Dynamic viscosity
η_I	[-]	Thermal efficiency
ε	[-]	Isentropic efficiency
λ	[W/(mK)]	Plate thermal conductivity
Subscripts		
b		bulk
cd		Condenser
CF		Cooling fluid
ev		Evaporator
HF		Heat carrier fluid
net		Net output
pc		Purchase cost
$pump$		Pump
$turb$		Turbine
WF		Working fluid
wl		Wall

Karellas et al. [4] studied the design of plate heat exchangers for supercritical ORCs based on theoretical models. A calculation and dimensioning method was proposed by discretising the heat exchanger in various segments and employing the Jackson correlation [5] to calculate the convective heat transfer coefficient in the supercritical region. Their results show that the performance of the ORC is increased without a disproportioned rise of installation costs due to larger heat exchangers. However, they conclude that a techno-economic investigation of real-scale supercritical ORCs is vital before drawing final conclusions.

Thermo-economic or techno-economic approaches in optimizing ORCs are scarce in literature. In Table 1 a general overview of papers is given which tackle the challenge of thermo-economic optimization of ORCs. In general there is a great variety in optimization strategies and level of detail in the component models.

Table 1 Overview of papers with as topic thermo-economic optimization.

Ref.	Objective function	Cycle
Hetteriarchi et al. (2007) [6]	- Total heat exchanger area on net power output [m^2/kWe].	SCORC
Cayer et al. (2010) [7]	- Relative cost per unit power [$€/kWe$].	TCORC
Shengjun et al. (2011) [8]	- Levelized energy cost [$$/kWh$].	SCORC,
	- Area per unit power [m^2/kWe].	TCORC
Quoilin et al. (2011) [9]	- Specific investment cost [$€/kWe$].	SCORC
Wang et al. (2012) [10]	- Combination of area per power output and heat recovery efficiency.	SCORC
Wang et al. (2013) [11]	- Area per unit power [m^2/kWe].	SCORC
Wang et al. ¹ (2013) [12]	- Exergy efficiency vs. total investment cost.	SCORC
Lecompte et al. (2013) [13]	- Specific investment cost [$€/kWe$].	SCORC
Pierobon et al. ¹ (2013) [14]	- Net present value vs. volume.	SCORC
	- Volume vs. thermal efficiency.	SCORC
Astolfi et al. (2013) [15]	- Plant total specific cost [$k€/kW$].	SCORC, TCORC

¹multi-objective optimization

From this overview only three works investigate the TCORC. Cayer et al. [7] studied transcritical power cycles for low temperature heat sources with working fluids R125, CO2 and ethane. The choice of performance indicator has a significant impact on the optimal operating condition and selected fluid. R125 has the best thermal efficiency and lowest relative cost per unit of power produced while ethane has the highest specific net power output. Astolfi et al. [15] compared the subcritical and transcritical ORC for the exploitation of medium-low temperature geothermal sources. They state, that as a general trend the configurations based on supercritical cycles, employing fluids with a critical temperature slightly lower than the temperature of the geothermal source, leads to the lowest electricity cost for most of the investigated cases. Also Shengjun et al. [8] compared the subcritical ORC and transcritical ORC for low temperature geothermal power generation. From the large selection of pure working fluids investigated, R125 in a transcritical power cycle was indicated

as cost effective solution for low-temperature geothermal ORC systems.

In the work of Astolfi et al. [15] the heat exchanger area multiplied with the overall heat transfer coefficient (UA) is taken as the sizing parameter for the heat exchangers cost function. This cost function is used both for the TCORC and SCORC case. In general the heat exchanger cost is directly linked to the heat exchanger area [16]. Therefore similar heat transfer coefficients are assumed for both the TCORC and SCORC. To incorporate the effect of the overall heat transfer coefficient, a cost function specifically derived for supercritical heat exchangers could be incorporated or the overall heat transfer coefficient should be calculated from correlations available in literature. Cayer et al. [7] and Shengjun et al. [8] are using the Petukhov-Kranoschekov [17] correlations to calculate the convective heat transfer coefficient in the supercritical state.

The above works have in common that they are all limited to single objective criteria. A specific weighing factor is given to the variables that form the single objective function. Therefore the valorisation potential of these variables are assumed fixed [15]. Introducing a multi-objective optimization provides more flexibility in post-processing and interpretation of the results at the expense of an increased computational time.

In this work a thermo-economic study of the transcritical ORC is presented with as focus waste heat recovery. Detailed heat exchanger models are derived which are used in the optimization strategy. In contrast to other works, a multi-objective optimization approach is developed. The objective criterion is net power output versus investment cost. The TCORC is further compared to the SCORC which was modelled in previous work [18].

DESCRIPTION OF THE TRANSCRITICAL CYCLE

The schematic of the TCORC layout and Ts diagram, useful to define the nomenclature, is given respectively in Figure 1a and Figure 1b.

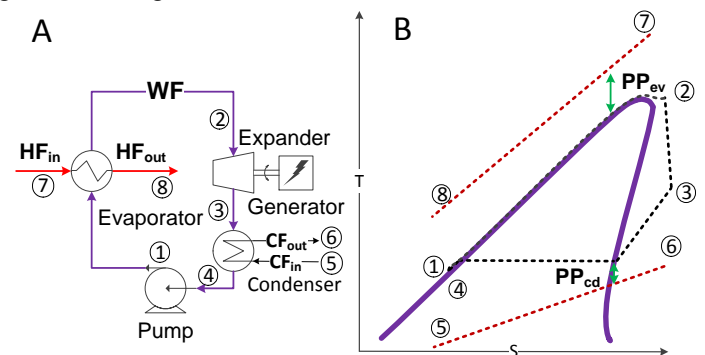


Figure 1 (a) schematic layout TCORC, (b) Ts diagram.

Similar as the SCORC, the TCORC consists of a pump, expander, evaporator and condenser. Because no phase change takes place in the TCORC, the evaporator is also called a vapor generator. The working fluid is heated to state 2 and subsequently expands to state 3 in the expander. The resulting shaft power is then converted to electricity by the generator. The superheated working fluid at the outlet of the turbine is

condensed to a saturated liquid in the condenser. The liquid working fluid is again pressurized by the pump, closing the cycle.

MODEL AND ASSUMPTIONS

In this section the modelling approach for the TCORC is discussed. The modelling strategy of the SCORC is identical and not repeated here for conciseness [18]. Firstly the waste heat recovery case and thermodynamics of the cycle are described. Secondly, the heat exchanger models are discussed and lastly, the cost models are briefly introduced.

Cycle assumptions

A low temperature waste heat recovery case is covered in this research. Waste heat with a temperature between 80 °C and 110 °C and a mass flow rate of 15 kg/s is available from a water cooling loop of a chemical process.

The ORC is evaluated assuming steady state conditions. Furthermore, the heat loss to ambient is neglected. Pumps and turbines are characterized by their isentropic efficiency. An overview of the fixed parameters and decision variables is given in Table 2.

Table 2 Fixed cycle parameters and decision variables.

Variable/parameter	Description	Value
PP _{ev}	Pinch point temperature difference evaporator [°C]	Optimized
PP _{cd}	Pinch point temperature difference condenser [°C]	Optimized
T _{CF,in}	Inlet temperature cooling fluid condenser [°C]	25
T ₂	Inlet temperature turbine	Optimized
p _{ev}	Evaporation pressure [Pa]	Optimized
p _{cd}	Condensation pressure [Pa]	Optimized
ε _{turbine}	Isentropic efficiency turbine [-]	0.7
ε _{pump}	Isentropic efficiency pump [-]	0.6
ΔT _{sub}	Temperature subcooling [°C]	3

A certain amount of subcooling is added to better comply with real life cycles. Condensers typically have a minimal flooding. In addition, a degree of subcooling is beneficial to avoid cavitation by the working fluid pump. However, the subcooling should be maintained low to achieve a high power output.

The selection of the working fluids is based on an extensive literature survey. R245fa is taken as reference working fluid for the SCORC due to its frequent use in commercial ORC installations. In literature, R125 [8, 19, 2] is recommended for low temperature transcritical operation. The selected fluids are not necessarily optimal for the discussed advanced cycles, but provide a good benchmark for further study and comparison. The thermophysical data is taken from REFPROP 9.0.

The pump and turbine are modelled by their isentropic efficiency:

$$\dot{W}_{pump} = \frac{(h_{pump,ex} - h_{pump,in})}{\epsilon_{pump}} \dot{m}_{WF} \quad (1)$$

$$\dot{W}_{turbine} = (h_{turbine,in} - h_{turbine,ex}) \epsilon_{turbine} \dot{m}_{WF} \quad (2)$$

The net power output is calculated as:

$$\dot{W}_{net} = \dot{W}_{turbine} - \dot{W}_{pump,ORC} - \dot{W}_{pump,HF} - \dot{W}_{pump,CF} \quad (3)$$

and the thermal efficiency is defined as:

$$\eta_I = \frac{\dot{W}_{net}}{\dot{Q}_{in}} \quad (4)$$

with \dot{Q}_{in} the heat input from the waste heat stream to the ORC evaporator.

Heat exchanger model

Both the condenser and evaporator are of the plate heat exchanger type. The fixed design values for the plate heat exchanger are given in Table 3. First, the model of the vapour generator will be discussed. The vapour generator is divided into 60 segments in order to account for changing fluid properties. This assures that the change in power output due to discretization errors is lower than 0.1% relative to the net power output. The log mean temperature difference (LMTD) is calculated for all of the segments:

$$\dot{Q}_i = \Delta T_{LMTD,i} F \cdot U_i \cdot A_i \quad (5)$$

With A the heat exchange area, F the configuration correction factor, and U the overall heat transfer coefficient:

$$\frac{1}{U_i} = \frac{1}{\alpha_{HF,i}} + \frac{1}{\alpha_{WF,i}} + \frac{t}{\lambda} \quad (6)$$

With α the convective heat transfer coefficient, t the plate thickness and λ the thermal conductivity of the plate. The energy balance requires that:

$$\dot{Q}_i = \dot{m}_{WF} (h_{WF,i+1} - h_{WF,i}) = \dot{m}_{HF} (h_{HF,i+1} - h_{HF,i}) \quad (7)$$

The product of number of passes (N) and paths (K) is equal for both sides:

$$N_{ev,WF} \cdot K_{ev,WF} = N_{ev,HF} \cdot K_{ev,HF} \quad (8)$$

The Petukhov-Kranoschekov [17] correlations are used to calculate the convective heat transfer coefficient and pressure drop in the supercritical state:

$$Nu = Nu_0 \left(\frac{\mu_b}{\mu_{wl}} \right)^{0.11} \left(\frac{k_b}{k_{wl}} \right)^{-0.33} \left(\frac{c_p}{c_{p,b}} \right)^{0.35} \quad (9)$$

$$Nu_0 = \frac{\left(\frac{f}{8} \right) Re_b \bar{Pr}}{12.7 \sqrt{\frac{f}{8} (\bar{Pr}^{2/3} - 1)} + 1.07} \quad (10)$$

$$f = (1.82 \log_{10} Re_b - 1.64)^{-2} \quad (11)$$

For the two-phase condensation process the correlations by Han et al. [20] are used. The single phase heat transfer and pressure drops are calculated from the well-known correlations of Martin [21].

Table 3 Fixed design parameters plate heat exchangers.

Variable	Description	Value
D_h	Hydraulic diameter [m]	0.0035
t	Plate thickness [m]	0.0005
β	Chevron angle [°]	45
λ	Plate thermal conductivity [W/(mK)]	13.56
p_{co}	Corrugation pitch [m]	0.007

Cost model

The cost correlations are based on the exponential scaling law and are taken from Turton et al. [16]. Data, from a survey of manufacturers during the period of May 2001 to September 2001, was fitted to the following equation:

$$\log_{10}(C_{pc}^0) = K_1 + K_2 \cdot \log_{10}(B) + K_3 * (\log_{10} B)^2 \quad (12)$$

B is the capacity or size parameters, K_1 , K_2 and K_3 are parameters of the curve fitting. For heat exchangers, B corresponds to the heat exchanger area, while for pumps and turbines this corresponds with respectively the power input and output. Correction factors F_p and F_m take into account the operating pressure and type of material used. Stainless steel is assumed for all equipment, therefore $F_m = 1$. The purchased cost of equipment is therefore given as:

$$C_{pc} = F_{pc} F_m C_{pc}^0 \quad (13)$$

These correlations were derived for a general Chemical Engineering Plant Cost Index (CPCI) of 397. To actualise the cost, a multiplication with $(CPCI_{2001}/CPCI_{2013})$ is made. The $CPCI_{2013}$ is set to the value of August 2013 (564.7). The cost functions are provided in dollar. To convert the values to euro, a conversion factor of 0.731 (19/12/2013) is taken into account. The total purchased cost of equipment is computed as:

$$C_{inv} = (C_d + C_{ev} + C_{turbine} + C_{pump}) \quad (14)$$

The SIC is defined as:

$$SIC = \frac{C_{inv}}{W_{net}} \quad (15)$$

OPTIMIZATION RESULTS

The transcritical cycle is optimized according to a set of predefined objectives. In the multi-objective approach presented here the net power output versus investment cost is taken as objective criterion. In Table 4 the decision variables and their range are given to fully define the optimization problem.

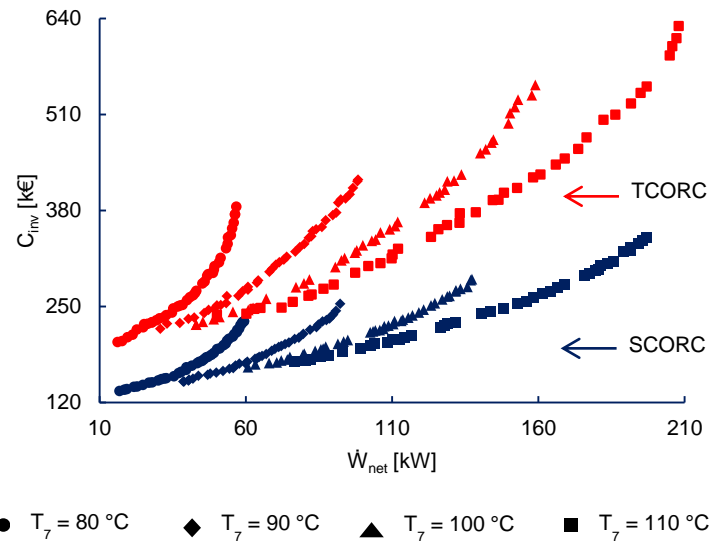
A genetic algorithm [22] optimizes the objectives in the set, resulting in a Pareto front. Working with a genetic algorithm has the benefit of searching for the global optimum while avoiding complex derivatives. An initial population of parameters is generated in the search area. The solutions are subsequently processed based on the objective criteria. The fittest are then selected to construct a new population based on crossover and mutation operations.

Table 4 Decision variables and range in the optimization problem.

Variable/Parameter	Description	Lower	Upper
PP_{ev}	Pinch point temperature difference evaporator [°C]	5	15
PP_{cd}	Pinch point temperature difference condenser [°C]	5	15
x	Evaporation pressure/supercritical pressure [-]	1.05	1.5
m_{wf}	Mass flow rate working fluid [kg/s]	10	25
$G_{ev, wf}$	Mass flux working fluid evaporator [kg/m ² /s]	10	200
$G_{cd, wf}$	Mass flux working fluid condenser [kg/m ² /s]	10	200
x	Ratio evaporation pressure on supercritical pressure [-]	1.05	1.5
N	Number of passes	1	4

Optimization with investment cost as objective function

To assess the influence of the heat carrier inlet temperature, T_7 is set to 80, 90, 100 and 110 °C. In Figure 2 the Pareto front for both the TCORC and SCORC is shown which results from the optimization process.

**Figure 2** Pareto front of investment cost (C_{inv}) versus net power output (\dot{W}_{net}) for SCORC and TCORC with heat carrier inlet temperatures T_7 of 80, 90, 100 and 110 °C.

For $T_7 = 80$ °C the cost for both the TCORC and SCORC rises sharply for higher net power output. While for higher heat carrier inlet temperatures the investment cost steadily increases with increased net power output. Furthermore, it is clear that the cost of the TCORC compared to the SCORC is up to 50% larger for a comparable power output. However, the maximum net power output can be considerably larger. Data of maximum \dot{W}_{net} , corresponding investment cost and minimum SIC is given in Table 5. For $T_7 = 100$ °C the maximum net power output of the TCORC is 16% larger than for the SCORC. In turn, this corresponds with an increased investment cost of 91%. As such, for each case, a profound financial analysis is necessary to account for the increased investment cost. For other heat

carrier inlet temperatures the increase in maximum net power output for the TCORC is less pronounced. We also see that the minimum SIC is highly dependent on the heat carrier inlet temperature and gradually approaches an asymptote.

In Figure 3 and Figure 4 the distribution of the components costs are plotted for respectively the SCORC and TCORC under $T_7 = 100$ °C. Most of the costs are lumped into the heat exchangers of the system. Especially the cost of the evaporator increases dramatically in the case of the TCORC. Looking at economies of scale a larger heat exchanger is not necessarily much costlier than a smaller one. This is also captured into the logarithmic laws of the cost functions. However in the low power ranges under consideration, the marginal cost of the heat exchanger is high. Therefore the increased heat exchange area needed for the TCORC results in a large cost. As a result, the TCORC is not necessarily the most cost-effective solution in small size, low temperature, installations.

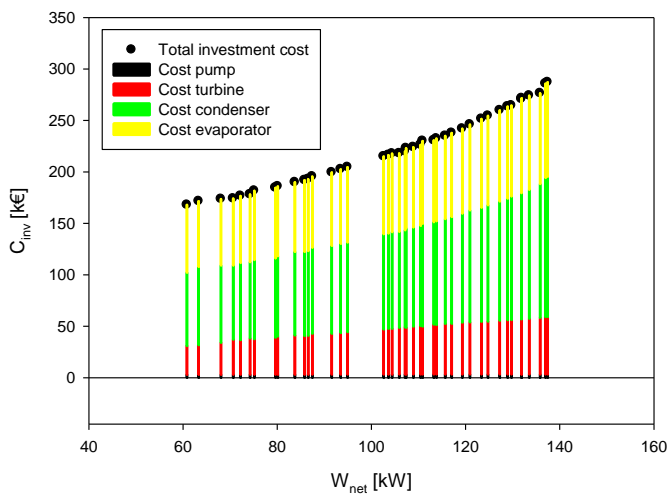


Figure 3 Distribution of component costs for the SCORC with heat carrier inlet temperature T_7 of 100 °C.

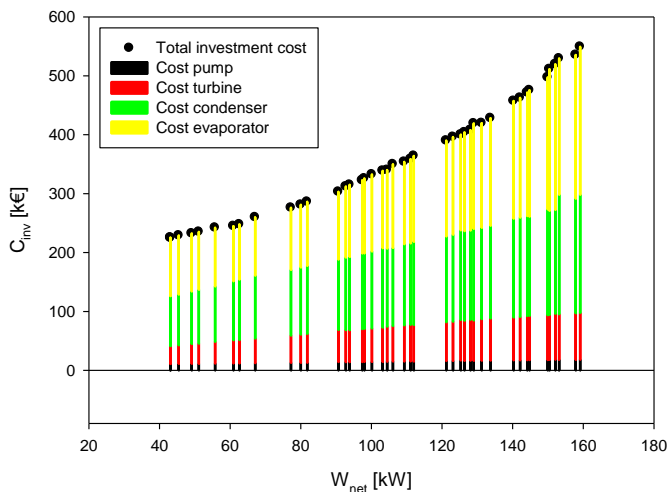


Figure 4 Distribution of component costs for the TCORC with heat carrier inlet temperature T_7 of 100 °C.

Table 5 Minimum SIC, maximum \dot{W}_{net} and corresponding C_{total} for the TCORC and SCORC with $T_7 = 80, 90, 100, 110$ °C.

T_7 [°C]	Min SIC [€/kWe]		Max \dot{W}_{net} [kW]		C_{total} (max \dot{W}_{net}) [k€]	
	SCORC	TCORC	SCORC	TCORC	SCORC	TCORC
80	3745	6045	59.5	56.8	229	384
90	2632	4146	92.3	98.5	254	421
100	2028	3189	137.4	159.0	287	550
110	1641	2662	197.0	211.0	343	643

CONCLUSION

Detailed models of the SCORC and TCORC for low temperature waste heat recovery are compared and optimized with a multi-objective algorithm. This results in the following interesting conclusions:

- The cost of the TCORC is up to 50% larger compared to the SCORC for identical net power outputs.
- The largest performance benefit for the TCORC is found for a waste heat inlet temperature of 100 °C.
- While the TCORC indicates an increased power output of 16%, the investment cost also increases with 91%.
- The heat exchangers account for the largest cost in the systems.
- The marginal cost for heat exchangers is high in small scale systems and works to a disadvantage for the TCORC.

ACKNOWLEDGMENTS

The results presented in this paper have been obtained within the frame of the IWT SBO-110006 project The Next Generation Organic Rankine Cycles (www.orcnext.be), funded by the Institute for the Promotion and Innovation by Science and Technology in Flanders. This financial support is gratefully acknowledged.

REFERENCES

- [1] G. Angelino and P. Colonna. Multicomponent working fluid for organic rankine cycles (orc). *Energy*, 23(6):449–463, 1998.
- [2] B. Saleh, G. Koglbauer, M. Wendland, and J. Fischer. Working fluids for low-temperature organic rankine cycles. *Energy*, 32(7):1210–1221, Jul 2007.
- [3] A. Schuster, S. Karellas, and R. Aumann. Efficiency optimization potential in supercritical organic rankine cycles. *Energy*, 35(2):1033–1039, Feb 2010.
- [4] S. Karellas, A. Schuster, and A. Leontaritis. Influence of supercritical ORC parameters on plate heat exchanger design. *Applied Thermal Engineering*, 33-34:70–76, Feb 2012.
- [5] J.D. Jackson and W.B. Hall. *Turbulent Forced Convection in Channels and Bundles*, volume 2. 1979.
- [6] H.D.M. Hettiarachchi, M. Golubovic, W. M. Worek, and Y. Ikegami. Optimum design criteria for an organic rankine cycle using low-temperature geothermal heat sources. *Energy*, 32(9):1698–1706, Sep 2007.
- [7] E. Cayer, N. Galanis, and H. Nesreddine. Parametric study and optimization of a transcritical power cycle using a low temperature source. *Applied Energy*, 87(4):1349–1357, Apr 2010.

- [8] Z. Shengjun, W. Huaixin, and G. Tao. Performance comparison and parametric optimization of subcritical organic rankine cycle (ORc) and transcritical power cycle system for low-temperature geothermal power generation. *Applied Energy*, 88(8):2740–2754, Aug 2011.
- [9] S. Quoilin, Declaye S., Tchanche B.F., and Lemort V. Thermo-economic optimization of waste heat recovery organic rankine cycles. *Applied Thermal Engineering*, 31:2885–2893, 2011.
- [10] Z.Q. Wang, N.J. Zhou, J. Guo, and X.Y. Wang. Fluid selection and parametric optimization of organic rankine cycle using low temperature waste heat. *Energy*, 40(1):107–115, Apr 2012.
- [11] Jiangfeng Wang, Zhequan Yan, Man Wang, Shaolin Ma, and Yiping Dai. Thermodynamic analysis and optimization of an (organic rankine cycle) ORc using low grade heat source. *Energy*, 49:356–365, Jan 2013.
- [12] Jiangfeng Wang, Zhequan Yan, Man Wang, Maoqing Li, and Yiping Dai. Multi-objective optimization of an organic rankine cycle (ORc) for low grade waste heat recovery using evolutionary algorithm. *Energy Conversion and Management*, 71:146–158, Jul 2013.
- [13] S. Lecompte, H. Huisseune, M. van den Broek, S. De Schampheleire, and M. De Paepe. Part load based thermo-economic optimization of the organic rankine cycle (ORC) applied to a combined heat and power (CHP) system. *Applied Energy*, 111:871–881, Nov 2013.
- [14] L. Pierobon, T. Nguyen, U. Larsen, F. Haglind, and B. Elmegaard. Multi-objective optimization of organic rankine cycles for waste heat recovery: Application in an offshore platform. *Energy*, 58:538–549, Sep 2013.
- [15] M. Astolfi, M. C. Romano, Paola B., and Macchi E. Binary ORC (organic rankine cycles) power plants for the exploitation of medium-low temperature geothermal sources - part b: Techno-economic optimization. *Energy*, xxx:1–12, 2013.
- [16] R. Turton, R. Bailie, W. Whiting, and J. Shaeiwitz. *Analysis, Synthesis and Design of Chemical Processes*. Pearson Education, 4 edition, 2013.
- [17] B.S. Petukhov, E.A. Krasnoshchekov, and Protopopov V.S. An investigation of heat transfer to fluid flowing in pipes under supercritical conditions. In *International developments in heat transfer, paper presented at the 1961 international heat transfer conference*, number 67, pages 569–578, University of Colorado, Boulder, CO, USA, January 1961. ASME.
- [18] S. Lecompte, M. van den Broek, and M. De Paepe. Optimal selection and sizing of heat exchangers for organic rankine cycles (orc) based on thermo-economics, under review. 15th International Heat Transfer conference (IHTC), 2014.
- [19] Huijuan Chen, D. Yogi Goswami, and Elias K. Stefanakos. A review of thermodynamic cycles and working fluids for the conversion of low-grade heat. *Renewable and Sustainable Energy Reviews*, 14(9):3059–3067, Dec 2010.
- [20] D.H. Han, K.J. Lee, and Y.H. Kim. The characteristics of condensation in brazed plate heat exchangers with different chevron angles. *Journal of the Korean Physical Society*, 43:66–73, 2003.
- [21] H. Martin. Economic optimization of compact heat exchangers. In *EF-Conference on Compact Heat Exchangers and Enhancement Technology for the Process Industries*, Banff, Canada, July 18–23 1999.
- [22] K. Deb. *Multi-Objective Optimization Using Evolutionary Algorithms*. John Wiley & Sons, 2001.